

Polarised Single-crystal Electronic Absorption Spectra of Tetraphenylarsonium Tetrahalogenonitridoruthenate(vi) Compounds and the Crystal and Molecular Structures of Tetraphenylarsonium Tetrabromonitridoruthenate(vi)

By David Collison, C. David Garner, and Frank E. Mabbs,* Department of Chemistry, Manchester University Manchester M13 P9L

Trevor J. King, Department of Chemistry, Nottingham University, Nottingham NG7 2RD

The polarised single-crystal electronic absorption spectra of $[\text{AsPh}_4][\text{RuNX}_4]$ ($X = \text{Cl}$ or Br) at room temperature and 5 K are reported in the range $10\,000\text{--}40\,000\text{ cm}^{-1}$. The spectra have been interpreted using the observed polarisation data in conjunction with a parameterised ligand-field model. The single-crystal structure of $[\text{AsPh}_4][\text{RuNBr}_4]$ has been determined by X-ray crystallography. The compound crystallises in the tetragonal space group $P4/n$, $a = b = 12.691(3)$, $c = 8.035(3)$ Å, $Z = 2$. The $[\text{RuNBr}_4]^-$ ion has $4mm$ (C_{4v}) symmetry with Ru-N 1.580(11), Ru-Br 2.453(1) Å, N-Ru-Br 104.25(3)°. The $[\text{AsPh}_4]^+$ cation has crystallographic $\bar{4}$ (S_4) symmetry, As-C 1.897(6) Å, C-As-C 104.64(40) and 111.95(21)°.

COMPOUNDS containing the MN^{n+} chromophore, where $M = \text{Ru}$ or Os , have been known for a number of years, but there are relatively little detailed absorption-spectral data for crystallographically characterised compounds available. However, the thin-film technique of Cowman *et al.*¹ on the tetra-*n*-butylammonium salts of $[\text{OsNX}_4]^-$ and $[\text{OsNX}_4(\text{OH}_2)]^-$ ($X = \text{Cl}$ or Br) and our previous² single-crystal polarised absorption spectral studies on $[\text{AsPh}_4][\text{OsNX}_4]$ ($X = \text{Cl}$, Br , or I) have provided the most detailed studies so far reported on these systems; there have been no similar studies on the ruthenium analogues. In view of this, and for comparison with the isostructural osmium compounds, we now report such a study on $[\text{AsPh}_4][\text{RuNX}_4]$ ($X = \text{Cl}$ or Br). In addition, we had determined the crystal structure of $[\text{AsPh}_4][\text{RuNBr}_4]$ which has not previously been reported.

EXPERIMENTAL

Preparation of the Compounds.— $[\text{AsPh}_4][\text{RuNCl}_4]$ was prepared from RuO_4^3 by the method of Griffith and Pawson.⁴ Crystals of this compound were grown by the slow evaporation of a methyl cyanide solution at room temperature in the dark (Found: C, 45.3; H, 3.1; Cl, 22.0; N, 2.2. Calc. for $\text{C}_{24}\text{H}_{20}\text{AsCl}_4\text{NRu}$: C, 45.0; H, 3.1; Cl, 22.2; N, 2.2%).

$[\text{AsPh}_4][\text{RuNBr}_4]$ was prepared by refluxing $[\text{AsPh}_4][\text{RuNCl}_4]$ (0.5 g) in MeCN-EtBr (1 : 10 v/v, 50 cm^3) for 8 d. The product was removed by filtration and crystals were grown by the slow evaporation of a MeCN solution at room temperature in the dark (Found: C, 34.8; H, 2.5; Br, 38.8; Cl, 0.0; N, 1.8. Calc. for $\text{C}_{24}\text{H}_{20}\text{AsBr}_4\text{NRu}$: C, 35.2; H, 2.4; Br, 39.1; N, 1.7%).

The i.r. spectra of these two compounds agreed with those reported previously.⁵

Electronic Absorption Spectra.—These were measured in the range $10\,000\text{--}40\,000\text{ cm}^{-1}$ for solutions at room-temperature (298 K) and for suitably thinned single crystals mounted on thin silica plates at room temperature and 5 K using equipment previously described.⁶ The orientations of the crystals were such that the electric vector of the incident beam could be polarised parallel to and perpendicular to the crystallographic c axis. The data obtained at 5 K are given in Tables 1 and 2, and in Figures 1 and 2 which also include the room-temperature spectra.

Single-crystal Structure.—*Crystal data.* $\text{C}_{24}\text{H}_{20}\text{AsBr}_4\text{NRu}$, $M = 817.9$, Tetragonal, $a = b = 12.691(3)$, $c = 8.035(3)$ Å, $U = 1\,294.2$ Å³, D_m (floatation) = 2.04, $Z = 2$, $D_c = 2.10\text{ g cm}^{-3}$, $F(000) = 776$, $\text{Mo-K}\alpha$ radiation, $\lambda =$

TABLE 1
Band positions (cm^{-1}) for the polarised single-crystal electronic absorption spectrum of $[\text{AsPh}_4][\text{RuNCl}_4]$ at 5 K *

z	Polarisation	Assignment	xy	Polarisation	Assignment	
17 490 m	z	$A_1(^3A_2)$				
17 680 m				17 700 m	$E(^3A_2)$	
17 810 m						
18 060 m						
18 240 m				18 220 m		
18 400 m						
18 570 m						
18 730 m						
18 930 m					18 910 m	
19 160 m						
19 270 (sh)						
19 340 m						
19 440 (sh)						
19 520 m						
19 630 (sh)						
19 740 m						
19 860 m						
19 940 (sh)						
20 020 m						
20 100 (sh)						
20 250 (sh)						
20 340 m			20 340 m	$E(^2E)$		
20 440 (sh)	z	$A_1(^2E)$				
20 520 m					1170	
20 750 m						
21 180 m						
21 470 m						
21 720 m					21 510 m	
22 230 m						1110
						1090
						22 620 m
					23 710 m	
			25 080	$A_2(^1A_2)$ vib		
29 630 (sh)						
30 090 (sh)						
			31 250 s	$E(^1E)$		
	z	$E(^1E)$ vib	31 970 s		720	
32 190 s					33 000 (sh)	1030
33 590 s			1400			960
					33 960 s	
			1110		34 420 s	
34 700 s						
35 710 s	1010					
36 280 s						
			37 040 s	C.T.		

* Assignment refers to the electronic excited-state label of the electronic transition from the $A_1(^1A_1)$ ground state; 'vib.' denotes that transition is vibronically allowed; C.T. = charge transfer; s = strong, m = medium, w = weak, (sh) = shoulder, br = broad, v = very.

0.7107 Å, $\mu(\text{Mo-K}\alpha) = 84.9 \text{ cm}^{-1}$, space group $P4/n$ from systematic absences, $hk0$ when $h + k \neq 2n$.

Preliminary unit-cell dimensions and space-group data were obtained from oscillation and Weissenberg photographs and refined on a Hilger and Watts four-circle diffractometer. The layers $0-10kl$ were examined for a needle-shaped crystal $ca. 0.4 \times 0.2 \times 0.2 \text{ mm}$ and 930 reflections with $I > 3\sigma(I)$ in the range $0 < 2\theta < 55^\circ$ were considered observed and used in the subsequent refinement.

TABLE 2

Band positions (cm^{-1}) for polarised single-crystal electronic absorption spectra of $[\text{AsPh}_4][\text{RuNBr}_4]$ at 5 K *

Wavenumber (cm^{-1})	Polarisation		Assignment
	z	xy	
16900w			$A_1(^3A_2)$
17280m			
18050(sh)		17330(sh)	$E(^1A_2)$
18890m		18760s	
		20020s	$E(^3E)$
20780m			$A_1(^3E)$
21430m			
		21460s	
		22040s	$A_2(^1A_2)$ vib.
22100m			
		25870s	$E(^1E)$

* See footnote to Table 1.

No corrections were made for absorption, anomalous dispersion, or secondary extinction. Data reduction and crystallographic calculations were carried out on the Nottingham I.C.L. 1906A computer using the Oxford University CRYSTALS programs. Atomic scattering factors were used as published.⁷ The structure was solved by normal heavy-atom, Patterson, and Fourier techniques and refined by least-squares procedures involving anisotropic temperature factors for all the non-hydrogen atoms. The hydrogen atoms were included in the refinement at fixed positions and each with a constant U_{iso} . The analysis converged at an R value of 0.055. Structure factors and thermal parameters are in Supplementary Publication No. SUP 23087 (11 pp.).*

RESULTS AND DISCUSSION

Crystal Structure.—The final atomic co-ordinates are listed in Table 3 and selected bond lengths and angles are in Table 4. The Ru-N bond length [1.580(11) Å] and the N-Ru-Br bond angle [104.25(3)°] compare well with the corresponding parameters [1.570(7) Å and 104.58(4)°] found in $[\text{AsPh}_4][\text{RuNCl}_4]$.⁵ Indeed, the M-N bond lengths in the compounds $[\text{AsPh}_4][\text{MNX}_4]$ show no significant differences throughout the series when M = Os, X = Cl, Br, or I and M = Ru, X = Cl or Br. Similarly, the M-X bond lengths show no significant change when M = Os or Ru for a given X, where X = Cl or Br. The N-M-X or X-M-X bond angles are also the same within the series M = Os or Ru and X = Cl or Br but the N-Os-I angle is significantly smaller and the I-Os-I angles significantly larger than the corresponding

* For details see Notices to Authors No. 7, *J. Chem. Soc., Dalton Trans.*, 1980, Index issue.

TABLE 3

Atomic co-ordinates for $[\text{AsPh}_4][\text{RuNBr}_4]$

	x/a	y/b	z/c
Ru(1)	0.2500	0.2500	0.122 4(1)
N(1)	0.2500	0.2500	-0.074(1)
Br(1)	0.409 78(7)	0.152 17(7)	0.197 5(1)
As(1)	0.2500	0.7500	0.0000
C(1)	0.132 0(5)	0.757 8(5)	0.144 3(8)
C(2)	0.054 3(5)	0.831 6(6)	0.117 8(9)
C(3)	-0.027 5(6)	0.840 9(7)	0.234(1)
C(4)	-0.027 6(7)	0.777 0(8)	0.373(1)
C(5)	0.048 0(7)	0.701 6(8)	0.394(1)
C(6)	0.129 3(6)	0.690 8(7)	0.282 0(9)
H(2)	0.056 9	0.877 5	0.016 9
H(3)	-0.085 3	0.898 2	0.214 1
H(4)	-0.087 1	0.782 3	0.455 6
H(5)	0.047 6	0.655 9	0.497 1
H(6)	0.183 1	0.632 7	0.293 4

angles in the chloro- and bromo-species. This is presumably due to the larger size of the iodide ligand.

In the $[\text{AsPh}_4]^+$ cation the As-C bond length [1.89(2)—1.91(1) Å] lies within the range found in a wide range of

TABLE 4

Bond distances (Å) and interbond angles (°) in $[\text{AsPh}_4][\text{RuNBr}_4]$

(a) Co-ordination about Ru			
Ru(1)-N(1)	1.580(11)	N(1)-Ru(1)-Br(1)	104.25(3)
Ru(1)-Br(1)	2.453(1)	Br(1)-Ru(1)-Br(1)'	151.51(6)
		Br(1)''-Ru(1)-Br(1)'''	86.53(1)
(b) In the $[\text{AsPh}_4]^+$ cation			
As(1)-C(1)	1.897(6)	C(1)-As(1)-C(1)'	104.63(40)
C(1)-C(2)	1.377(10)	C(1)''-As(1)-C(1)'''	111.95(21)
C(1)-C(6)	1.396(10)	As(1)-C(1)-C(2)	120.45(52)
C(2)-C(3)	1.398(10)	As(1)-C(1)-C(6)	118.19(54)
C(3)-C(4)	1.385(13)	C(2)-C(1)-C(6)	121.27(66)
C(4)-C(5)	1.365(14)	C(1)-C(2)-C(3)	119.09(73)
C(5)-C(6)	1.376(11)	C(2)-C(3)-C(4)	119.38(78)
		C(3)-C(4)-C(5)	120.57(72)
		C(4)-C(5)-C(6)	121.10(81)
		C(5)-C(6)-C(1)	118.47(80)

isomorphous systems.^{2,7-12} The valency angles at the arsenic atom [104.63(40) and 111.95(21)°] show deformations from ideal tetrahedral values. These values suggest a larger difference in bond angles at the arsenic atom in $[\text{AsPh}_4][\text{RuNBr}_4]$ compared with the other systems, but they are within the range observed previously [105.1(5)—111.7(3)°]. Other bond lengths and valency angles in the cation show no unusual features.

Electronic Absorption Spectra.—Before discussing the spectra, it is worth summarising the predicted order of the excited states for $[\text{RuNX}_4]^-$ centres based on an extrapolation of the parameters used to account for the corresponding spectra of $[\text{OsNX}_4]^-$. If we assume that the d orbital splittings are not substantially different from ruthenium to osmium, then the major changes in the parameters will be an increase in the interelectron repulsion parameter and a decrease in the spin-orbit coupling constant.¹³ Making these changes we found that the calculated relative order of the excited states was $A_1(^3A_2) < E(^3A_2) < E(^3E) < A_1(^3E) < A_2(^1A_2) < E(^1E) < E(^3B_2)$. The changes in the positions of states within the manifold compared to that in $[\text{OsNCl}_4]^-$ [$E(^3E) < A_1(^3E) < E(^3A_2) < A_1(^3A_2) < A_2(^1A_2) < E(^1E)$]

were largely determined by the increase in the interelectron repulsion parameters. The decrease in the spin-orbit coupling constant reduced the separations between states within a spin-orbit multiplet, and at the same time reduced the mixing between spin-orbit terms of the same symmetry. One consequence of these

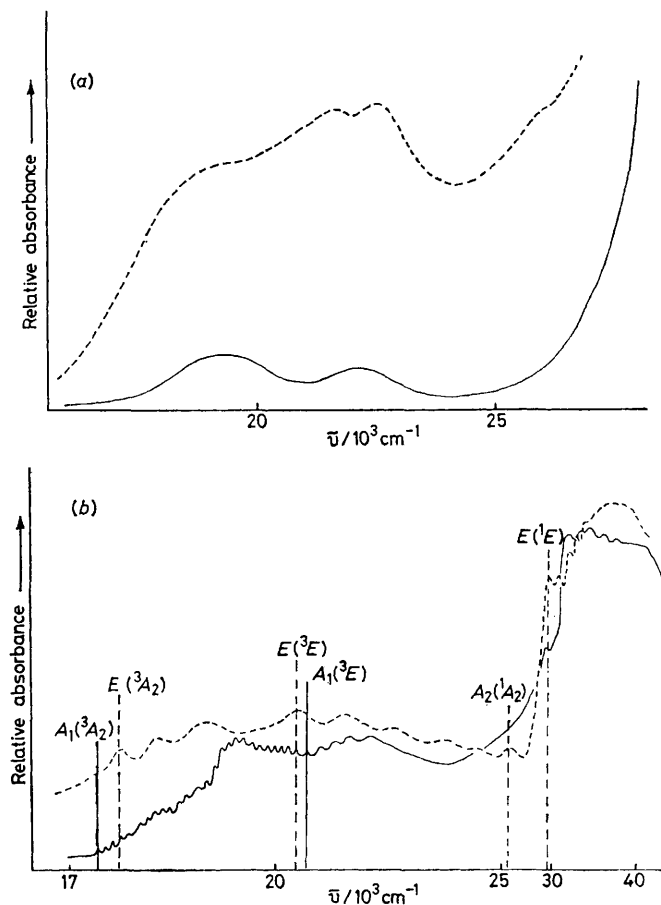


FIGURE 1 Polarised single-crystal electronic absorption spectrum of $[\text{AsPh}_4][\text{RuNCl}_4]$ at (a) 298 K, (b) 5 K; z polarisation (—), xy polarisation (-----)

changes is likely to be a reduction in the energy separations between the bands in the electronic absorption spectrum.

$[\text{AsPh}_4][\text{RuNCl}_4]$. The single-crystal electronic absorption spectrum at room temperature [Figure 1(a)] up to *ca.* $25\,000\text{ cm}^{-1}$ was more intense in xy than in z polarisation. Above *ca.* $25\,000\text{ cm}^{-1}$ the spectra in both polarisations were too intense to record. In z polarisation the spectrum consisted of two broad weak features centred on *ca.* $19\,000$ and $22\,000\text{ cm}^{-1}$, whilst in xy polarisation there was a broad absorption upon which were superimposed a shoulder at *ca.* $18\,000$, maxima at *ca.* $22\,000$ and $23\,000$, and a second shoulder at *ca.* $26\,000\text{ cm}^{-1}$.

Cooling the crystals to 5 K reduced the intensities in both polarisations and enabled some bands to be observed above $25\,000\text{ cm}^{-1}$. Two crystal thicknesses

were used to obtain these spectra, the thicker one being used for z polarisation. The data for the two thicknesses were scaled to maintain the relative intensities of the two polarisations. The z -polarised spectrum starts with a band at $17\,490\text{ cm}^{-1}$ which is followed by a large number of features with spacings varying between 110 and 230 cm^{-1} . There is a break in this pattern of splittings to one with much larger intervals starting with a band at $20\,750\text{ cm}^{-1}$. These two regions of the spectrum are

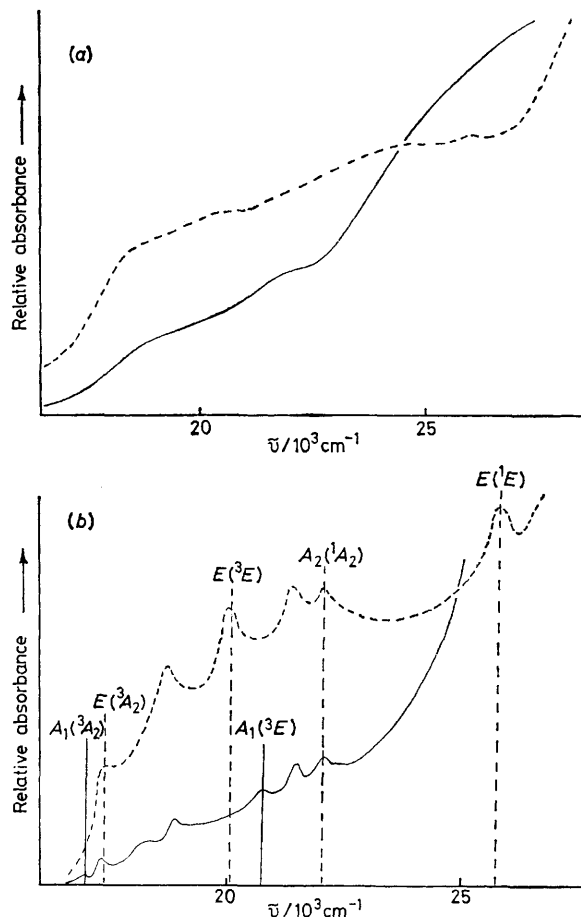


FIGURE 2 Polarised single-crystal electronic absorption spectrum of $[\text{AsPh}_4][\text{RuNBr}_4]$ at (a) 298 K, (b) 5 K; z polarisation (—), xy polarisation (-----)

covered by the two broad maxima in z polarisation observed at room temperature. For these reasons, we propose that the band at $17\,490\text{ cm}^{-1}$ is the origin of the $A_1(1A_1) \rightarrow A_1(3A_2)$ transition whilst that at $20\,750\text{ cm}^{-1}$ is the origin of the $A_1(1A_1) \rightarrow A_1(3E)$ transition. The xy -polarised spectrum consisted of eight broad bands of medium intensity up to *ca.* $25\,000\text{ cm}^{-1}$, followed by a series of bands superimposed on a rising background. Because of the lack of well resolved vibrational fine structure the assignment of the xy -polarised spectrum was not as clear cut as for the osmium analogue. Our proposed assignment is that the first band in this polarisation at $17\,700\text{ cm}^{-1}$ is the origin of the $A_1(1A_1) \rightarrow E(3A_2)$ transition. The series of bands with separations

of ca. 1 100 cm^{-1} originating at 20 340 cm^{-1} was assigned to the $A_1(^1A_1) \rightarrow E(^3E)$ transition, whilst the four-membered progression of average spacing 815 cm^{-1} , originating at 31 970 cm^{-1} , was assigned to the $A_1(^1A_1) \rightarrow E(^1E)$ transition. The band at 25 080 cm^{-1} , which has no counterpart in z polarisation, was assigned to the (vibronically allowed) $A_1(^1A_1) \rightarrow A_2(^1A_2)$ transition on the grounds that the ligand-field calculation placed it between the $A_1(^3E)$ and $E(^1E)$ states *and* that it is forbidden in z polarisation due to the lack of vibrations of A_2 symmetry in these C_{4v} anions. The parameterised ligand-field calculations showed this assignment to be internally consistent, and the least-squares fit is given in Table 5. The calculations

TABLE 5

Best-fit ligand-field parameters for $[\text{AsPh}_4][\text{RuNX}_4]$

Excited states and ligand-field parameters	Band energies $\ast/10^3 \text{ cm}^{-1}$			
	X = Cl		X = Br	
	Obs.	Calc.	Obs.	Calc.
$A_1(^3A_2)$	<i>17.49</i>	17.63	<i>16.90</i>	17.18
$E(^3A_2)$	<i>17.70</i>	17.64	<i>17.33</i>	17.18
$B_1(^3E)$		19.85		19.52
$B_2(^3E)$		19.86		19.53
$E(^3E)$	<i>20.34</i>	20.31	<i>20.02</i>	20.07
$A_2(^3E)$		20.62		20.21
$A_1(^3E)$	<i>20.75</i>	20.80	<i>20.78</i>	20.72
$A_2(^1A_2)$	<i>25.08</i>	25.06	<i>22.04</i>	21.95
$E(^1E)$	<i>31.25</i>	31.30	<i>25.87</i>	25.90
$B_1(^3B_2)$		41.66		50.68
$E(^3B_2)$		41.69		50.69
$B_2(^1B_2)$		53.92		56.95
$D_1/10^3 \text{ cm}^{-1}$		36.80		28.70
$D_2/10^3 \text{ cm}^{-1}$		28.60		23.70
$D_3/10^3 \text{ cm}^{-1}$		60.00		60.00
F_2/cm^{-1}	1 144.0		553.5	
F_4/cm^{-1}		104.0		61.5
$\xi_{\text{Ru}}/\text{cm}^{-1}$		800.0	1 000.0	
F_2/F_4		11.0		9.0
$\delta(\%)$		0.6		0.9
Ru-X/ \AA		2.310		2.453

\ast Band positions in italics were those assigned and used on the ligand-field fitting procedure.

showed that the forbidden transitions to the $B_1(^3E)$, $B_2(^3E)$, and $A_2(^3E)$ states are very close to the allowed transitions to the $E(^3E)$ and $A_1(^3E)$ states. Thus, because of the lack of resolution, we cannot confirm the presence of bands attributable to these forbidden transitions.

$[\text{AsPh}_4][\text{RuNBr}_4]$. The single-crystal polarised electronic absorption spectrum at 5 K is shown in Figure 2 and Table 2. The intensity of the xy -polarised spectrum is greater than that for z polarisation. However, compared with the chloro-analogue there is no readily recognisable vibrational fine structure, presumably due, at least in part, to the lower frequencies for those vibrations involving displacement of the bromine atoms. Also, compared to $[\text{RuNCl}_4]^-$ there is a greater absorption tailing into the visible region, presumably due to in-plane ligand-to-metal charge-transfer bands moving to lower energy for bromide *versus* chloride ligands.

Because of the lack of vibrational fine structure and obvious polarisation the assignment of this spectrum is

less clear cut than that of $[\text{RuNCl}_4]^-$, or the $[\text{OsNCl}_4]^-$ or $[\text{OsNBr}_4]^-$ analogues. Our assignment relies on the results of the parameterised ligand-field calculation using parameters which change from those used to fit the chloro-analogue in the anticipated manner, *i.e.* a decrease in D_1 , D_2 , and F_2 . The preferred assignment based on what appear to be reasonable values of D_1 , D_2 , F_2 , and F_4 compared with $[\text{RuNCl}_4]^-$ and $[\text{OsNX}_4]^-$ is summarised in Figure 2 and Table 5. However, this assignment leaves a number of strong features, particularly those at 18 700 and 21 460 cm^{-1} in the xy -polarised spectrum, unassigned. The assignment of the first four features in the xy polarised spectrum to transitions to $E(^3A_2)$, $E(^3E)$, $A_2(^1A_2)$, and $E(^1E)$ respectively can be accommodated by the ligand-field calculation. However, this requires an unrealistically large decrease in the interelectronic repulsion parameters ($F_2 = 108.0 \text{ cm}^{-1}$, $F_4 = 36.0 \text{ cm}^{-1}$) such that $F_2 < 5F_4$, and for these reasons we consider this assignment inappropriate.

Ligand-field Parameters.—The trend in the values of D_1 and D_2 is similar to that observed for the osmium analogues, *i.e.* a decrease in changing from chloride to bromide. We propose that the explanation for this trend in terms of increasing metal-in-plane-ligand covalency also applies to the ruthenium complexes. The unexpected feature is the close similarity of the values of D_2 between the ruthenium and osmium analogues. Since D_2 represents the splitting between d_{xy}^* and $d_{x^2-y^2}^*$, *i.e.* $10Dq$ in crystal-field terms, the often quoted trend¹⁴ of a 25–40% increase in this splitting between successive members of a transition-metal group is not generally applicable to these complexes.

The interelectron repulsion parameter, F_2 , decreases on changing from chloride to bromide in a similar manner to that found for the osmium analogues. Indeed, the actual values of F_2 for corresponding ruthenium and osmium complexes are very nearly the same. In contrast to this, the values of F_4 for the ruthenium complexes are significantly higher compared with F_4 for the corresponding osmium analogues. However, in the ruthenium complexes there is a decrease in F_4 on going from chloride to bromide. This contrasts with a slight increase in F_4 in the corresponding osmium system, which is then followed by a decrease on co-ordination of iodide. By comparison with the osmium complexes, this suggests that the effect on F_4 of decreasing z_{off} , *versus* increasing bond length now dominates at bromide rather than at iodide as in the osmium complexes.

Although it is difficult to interpret the magnitudes of F_2 and F_4 for individual complexes, the relative values for corresponding ruthenium and osmium analogues may be qualitatively correlated with theoretical predictions. Thus it is known that complexation should decrease both F_2 and F_4 from their free-ion values.¹⁵ However, F_2 is affected by the ligands more than is F_4 .¹⁶ The free-ion value of F_4 for the $4d$ orbitals of Ru^{n+} would be expected to be greater than that of the $5d$ orbitals of the corresponding osmium ion. Thus it seems possible that the F_2 values of corresponding ruthenium and osmium

complexes could be similar, whilst the F_4 values remain larger for the ruthenium analogue.

We thank the S.R.C. for financial support.

[1/110 Received, 26th January, 1981]

REFERENCES

- ¹ C. D. Cowman, W. C. Trogler, K. R. Mann, C. K. Poon, and H. B. Gray, *Inorg. Chem.*, 1976, **15**, 1747.
- ² D. Collison, C. D. Garner, F. E. Mabbs, J. A. Salthouse, and T. J. King, preceding paper.
- ³ H. Nakata, *Tetrahedron*, 1963, **19**, 1959.
- ⁴ W. P. Griffith and D. Pawson, *J. Chem. Soc., Dalton Trans.*, 1973, 1314.
- ⁵ R. Collin, W. P. Griffith, and D. Pawson, *J. Mol. Struct.*, 1975, **5**, 83.
- ⁶ D. L. McFadden, A. T. McPhail, C. D. Garner, and F. E. Mabbs, *J. Chem. Soc., Dalton Trans.*, 1975, 263.
- ⁷ 'International Tables for X-Ray Crystallography,' Kynoch Press, Birmingham, 1962, vol. 3.
- ⁸ F. L. Phillips and A. C. Skapski, *Acta Crystallogr.*, 1975, **B31**, 2667.
- ⁹ F. L. Phillips and A. C. Skapski, *J. Cryst. Mol. Struct.*, 1975, **5**, 83.
- ¹⁰ F. L. Phillips, A. C. Skapski, and M. J. Withers, *Transition Met. Chem.*, 1975, **1**, 28.
- ¹¹ B. Knopp, K-P Lörcher, and J. Strähle, *Z. Naturforsch.*, 1977, **B32**, 1361.
- ¹² C. D. Garner, L. H. Hill, F. E. Mabbs, D. L. McFadden, and A. T. McPhail, *J. Chem. Soc., Dalton Trans.*, 1977, 853, 1202.
- ¹³ B. Gahan, C. D. Garner, L. H. Hill, F. E. Mabbs, K. D. Hargreaves, and A. T. McPhail, *J. Chem. Soc., Dalton Trans.*, 1977, 1726.
- ¹⁴ B. N. Figgis and J. Lewis in 'Progress in Inorganic Chemistry,' ed. F. A. Cotton, Interscience, New York, 1964.
- ¹⁵ See for example F. A. Cotton and G. Wilkinson, 'Advanced Inorganic Chemistry,' 3rd edn., Interscience, New York, 1972, ch. 20.
- ¹⁶ M. Gerloch and R. C. Slade, 'Ligand Field Parameters,' Cambridge University Press, 1973, ch. 9.